**Naval Research Laboratory**

Washington, DC 20375-5000



NRL Memorandum Report 6859

# Frequency-Independent and Frequency-Dependent Polymer Transitions on Flexural Plate Wave Devices and Their Effects on Vapor Sensor Response Mechanisms

JAY W. GRATE, STUART W. WENZEL* AND RICHARD M. WHITE*

*Surface Chemistry Branch*
*Chemistry Division*

**Berkeley Sensor & Actuator Center,*
*Department of Electrical Engineering and Computer Sciences*
*and the Electronics Research Laboratory,*
*University of California, Berkeley, CA 94720*

August 10, 1991

# REPORT DOCUMENTATION PAGE

Form Approved
OMB No 0704-0188



| 1. AGENCY USE ONLY (Leave blank) | 2. REPORT DATE | 3. REPORT TYPE AND DATES COVERED |
|---|---|---|
| | 1991 August 10 | |

**4. TITLE AND SUBTITLE**
Frequency-Independent and Frequency-Dependent Polymer Transitions on Flexural Plate Wave Devices and Their Effects on Vapor Sensor Response Mechanisms

**5. FUNDING NUMBERS**
61-1639-E1

**6 AUTHOR(S)**
Jay W. Grate, Stuart W. Wenzel,* and Richard M. White*

**7. PERFORMING ORGANIZATION NAME(S) AND ADDRESS(ES)**
Chemistry Division
Naval Research Laboratory
Washington, DC 20375-5000

**8. PERFORMING ORGANIZATION REPORT NUMBER**
NRL Memorandum Report 6859

**9. SPONSORING/MONITORING AGENCY NAME(S) AND ADDRESS(ES)**
Office of Naval Technology
Naval Surface Warfare Center
Dahlgren, VA 22448-5000

**10. SPONSORING/MONITORING AGENCY REPORT NUMBER**

**11. SUPPLEMENTARY NOTES**
* Berkeley Sensor & Actuator Center, Department of Electrical Engineering and Computer Sciences and the Electronics Research Laboratory, University of California, Berkeley, CA 94720

**12a. DISTRIBUTION/AVAILABILITY STATEMENT**
Approved for public release; distribution unlimited.

**12b. DISTRIBUTION CODE**

**13. ABSTRACT** *(Maximum 200 words)*

The flexural plate wave device is capable of sensing transition behaviors of homogeneous amorphous polymers applied as thin films to its surface. The changes in polymer properties at the static glass transition temperature are sensed as a change in slope of the frequency-temperature plot. Frequency-dependent relaxation properties are detected with a sigmoidal change in slope of the frequency-temperature plot and a minimum in signal amplitude. The transitions observed using poly(vinyl acetate), poly(t-butyl acrylate), poly(isobutylene) and poly(vinyl propionate) are correlated with the properties of these polymers known by independent methods. The responses of the flexural plate wave device at 5 MHz are in accord with the results of ultrasonic experiments at similar frequencies. The effects of polymer relaxation processes on the performance and selection of sorbent polymers on acoustic vapors sensors are discussed.

| 14. SUBJECT TERMS | | | 15. NUMBER OF PAGES |
|---|---|---|---|
| Flexural plate wave,<br>Polymer,<br>Relaxation, | Sensor,<br>Class transition<br>Ultrasonic | Surface acoustic wave | 45<br>16. PRICE CODE |

| 17. SECURITY CLASSIFICATION OF REPORT | 18. SECURITY CLASSIFICATION OF THIS PAGE | 19. SECURITY CLASSIFICATION OF ABSTRACT | 20. LIMITATION OF ABSTRACT |
|---|---|---|---|
| Unclassified | Unclassified | Unclassified | Unlimited |

## CONTENTS




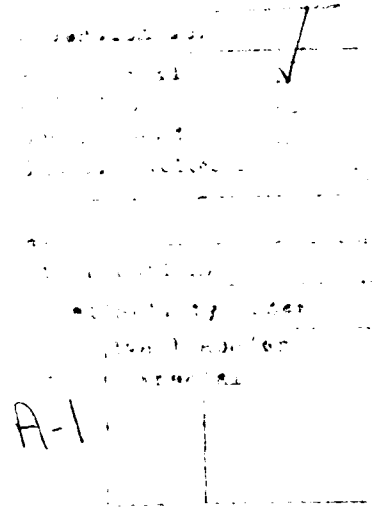

# FREQUENCY-INDEPENDENT AND FREQUENCY-DEPENDENT POLYMER TRANSITIONS ON FLEXURAL PLATE WAVE DEVICES AND THEIR EFFECTS ON VAPOR SENSOR RESPONSE MECHANISMS

## INTRODUCTION

Flexural plate wave (FPW) devices have demonstrated potential for a variety of sensing applications (1-9). As gravimetric sensors, these devices offer high mass sensitivity at low operating frequencies. In the gas phase, vapors can be detected in a manner analogous to other piezoelectric sorption detectors such as quartz crystal microbalance (QCM) vapor sensors or surface acoustic wave (SAW) vapor sensors (10-19). In this application a thin sorbent film, often a polymer, is applied to the device surface to collect and concentrate vapor molecules from the gas phase. Flexural plate wave devices also function in the liquid phase or with aqueous gels applied (1), and thus have clear potential for use as biosensors. In addition, physical properties of liquids such as density and viscosity can be sensed (4). Another interesting property of these devices is their ability to pump fluids or transport granular solids (2). A schematic diagram of the flexural plate wave device is shown in Figure 1. The theory and operation of these devices have been described in the papers cited above.

We have briefly reported that FPW devices are capable of sensing changes in polymer physical properties that occur at the glass transition temperature (9). There are actually a variety of polymer properties that change at the glass transition, a variety of physical methods to measure the glass transition, and, indeed, a variety of ways to define "glass transition" (20-30). Moreover, transition temperatures vary with the method of measurement and the rate of the measurement. This is a potentially confusing situation to the uninitiated. In this paper we will focus on two types of transitions which are both referred to as glass transitions. Changes in polymer thermal expansion rates, which are *frequency-independent*, are associated with a transition sometimes referred to as the static or dilatometric glass transition (29-33). We will refer to the temperature of this transition as the $T_g$, and sometimes more loosely to the transition itself as the $T_g$. Transitions associated with polymer relaxation processes under dynamic conditions are referred to as dynamic glass transitions. The transition temperatures associated with relaxation processes are highly *frequency-dependent* (24-30). We will use $T_\alpha$ to denote the transition

Manuscript approved June 18, 1991.

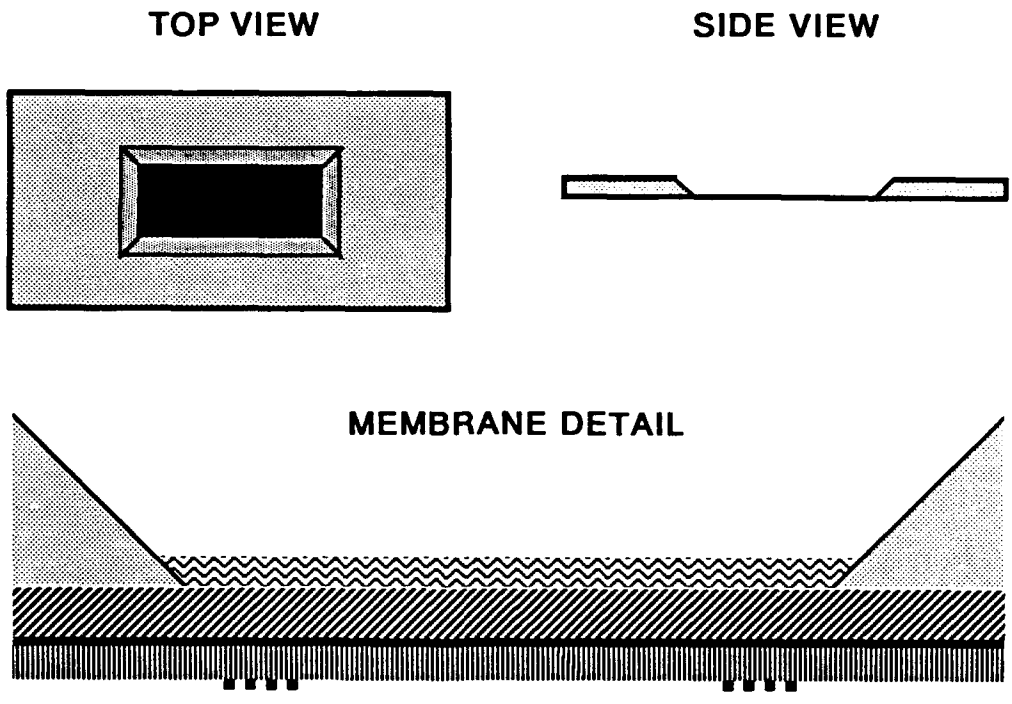


Figure 1. Schematic diagrams of a flexural plate wave device. In the top view, the membrane is shown in black at the bottom of the etch pit. The interdigital transducers are on the opposite side of the membrane, and thus are not shown in this view. The side view and membrane detail show cross-sections through the center. The structures in the membrane detail (shown with exaggerated vertical scale) are, from top to bottom, the supporting silicon substrate on the sides, the polymer overlayer, the silicon nitride layer, the aluminum ground plane, the piezoelectric zinc oxide layer, and the aluminum interdigital transducers.

temperature associated with the primary relaxation of polymer chain segments, as we describe in more detail below. At low frequencies, i.e., a few Hz or less, $T_\alpha$ is close to $T_g$. As the measurement frequency is increased, $T_\alpha$ increases while $T_g$ remains the same, giving rise to two separate transition temperatures.

Changes in the rate of polymer thermal expansion are measured experimentally by dilatometry. The upper plot in Figure 2 illustrates the results of such an experiment on an amorphous polymer. The coefficient of thermal expansion determined from the slope of the volume-temperature plot is constant up to $T_g$, at which point it abruptly increases by a factor of ca. 2 to 3 (typically). The occupied volume of the polymer chains is believed to increase at the same rate below and above $T_g$. The increase in the rate of thermal expansion above $T_g$ is attributed primarily to increases in free volume. As the free volume increases, density decreases, thermal segmental chain motion increases, the polymer softens from a glass to a rubber, the modulus decreases, and the viscosity decreases. (In this context modulus refers to the storage or elastic modulus, and this will be the meaning of modulus throughout the paper unless noted otherwise. In simpler terms, modulus refers to the stiffness of the material.) Additional properties that change at $T_g$ are the rates of vapor diffusion in the polymer (which increase as the free volume increases) and the heat capacity. Thermal methods such as differential scanning calorimetry (DSC) and differential thermal analysis (DTA) are convenient methods to determine the $T_g$ values of polymers.

The change in the rate of polymer thermal expansion associated with the glass transition can also be observed in ultrasonic studies (29-33). This phenomenon is illustrated in the lower plot of Figure 2. As the temperature is raised acoustic velocities in an amorphous polymer mirror changes in polymer volume with temperature; decreases in the acoustic velocity with temperature become steeper at $T_g$. This effect is believed to be due to the decreases in modulus that occur as the polymer expands above $T_g$. Modulus is strongly dependent on density (30). It should be noted that acoustic studies of polymers are dynamic experiments where the sound pressure induces strains in the polymer at the sonic frequency. Nevertheless, the change in the rate of polymer thermal expansion occurs at the static glass transition temperature. Thus, the transition in thermal expansion rates is frequency-independent.

Polymer relaxation processes are typically examined by dynamic mechanical analysis (DMA), ultrasonic methods, or dielectric methods (25-30). The primary relaxation associated with motions of polymer chain segments is referred to as the $\alpha$ relaxation. The temperature of the transition associated with this relaxation, or more simply stated the "relaxation temperature", is then $T_\alpha$. Additional relaxations associated with the motions of

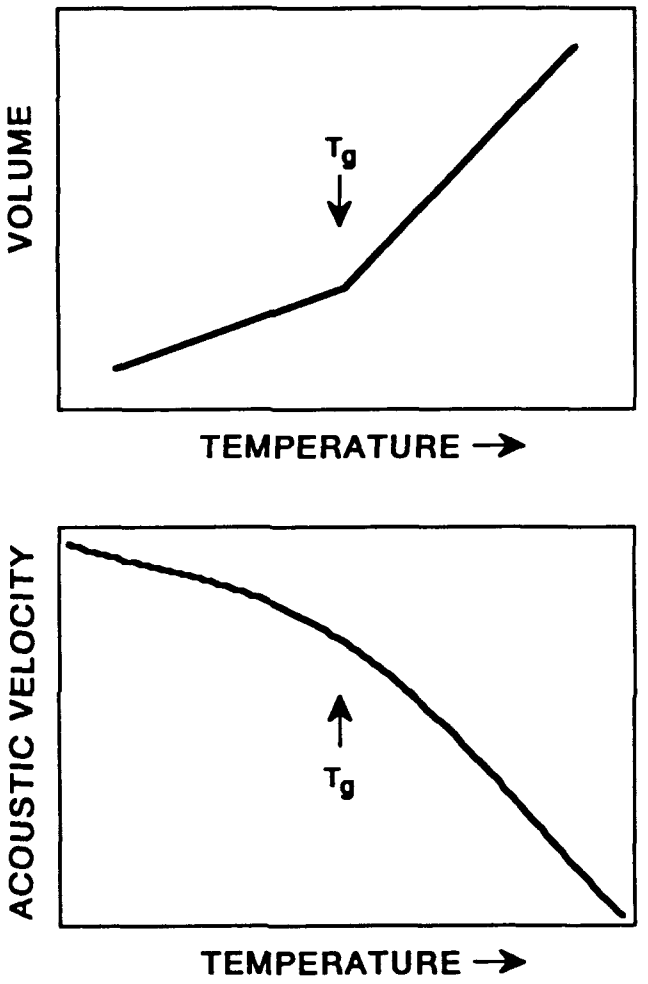


Figure 2. Plots illustrating the static glass transition temperature of an amorphous polymer. The upper plot shows the increase in the rate of thermal expansion as it would be measured by dilatometry. The lower plot shows how the expansion of the polymer influences the acoustic velocity in an ultrasonic experiment.

groups attached to the polymer backbone may occur at temperatures below $T_\alpha$, and these are referred to as $\beta$ and $\gamma$ relaxations. Large changes in the modulus and viscosity, as measured by dynamic methods, are associated with the $\alpha$ relaxation. Consequently, it is this $\alpha$ relaxation that gives rise to the dynamic glass transition. (In the literature, the distinction between the static and dynamic glass transitions is not always made clear, and both may be denoted by $T_g$. In this manuscript, we will avoid this confusing practice by using $T_g$ only when referring to the static glass transition temperature, and $T_\alpha$ when referring to the temperatures of relaxation processes under dynamic conditions.)

In DMA, a periodic stress at a particular frequency is applied to the polymer, inducing periodic strains (or vice versa). If the polymer is amorphous and above its $T_g$, the strains relax by thermal motion at a rate that is characteristic of the polymer, the experimental temperature, and the free volume in that particular polymer at that particular temperature. If the characteristic relaxation time is much shorter than the period between stresses, the measured modulus is that of a soft, rubbery material. If the periodic stresses occur faster than the material can relax, then the measured modulus will be that of a stiff glass. For a given polymer, the shorter the period between stresses (or the higher the frequency), the higher the temperature required for the the polymer to relax at that frequency. These phenomena are the basis for the time-temperature superposition principle (25-28). For our purposes, in simple terms, the effect of increasing the frequency is to increase the temperature of the relaxation, $T_\alpha$.

The upper plot in Figure 3 illustrates typical results from DMA of an amorphous polymer above its $T_g$. The elastic modulus and the loss tangent are plotted as a function of temperature at a constant frequency. The elastic modulus represents energy storage and is also referred to as the storage modulus. The loss tangent is the ratio of the loss modulus to the storage modulus; it indicates energy dissipation. (Follow the bold lines for this discussion.) As the temperature rises and the polymer passes through the relaxation temperature, $T_\alpha$, the elastic modulus decreases significantly. At the same time the loss tangent reaches a maximum. If the frequency of the experiment illustrated with bold lines in Figure 3 were reduced, then both curves would shift to the left and the transition would occur at a lower temperature. This is shown with the plain line curves. Alternatively, keeping the frequency constant, plasticizing the polymer material by dissolving lower molecular weight molecules in it would also shift the curves to the left and decrease $T_\alpha$.

The lower plot in Figure 3 illustrates typical results from an ultrasonic experiment on an amorphous polymer at temperatures above the $T_g$ (29,30). Acoustic velocity and acoustic absorption are plotted as a function of temperature, keeping the acoustic frequency

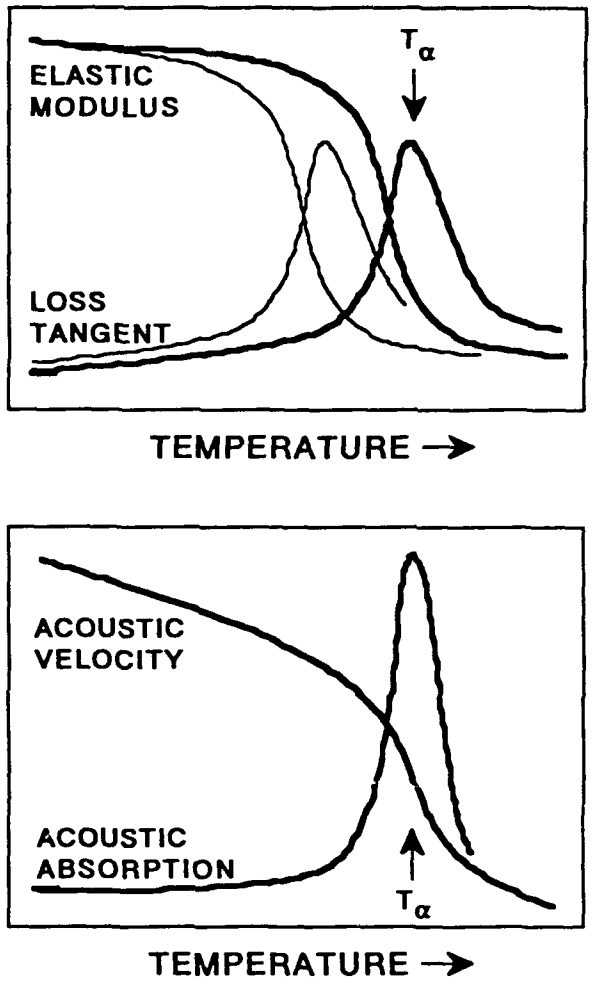


Figure 3. Plots illustrating the dynamic glass transition temperature of an amorphous polymer. The upper plot shows the results from DMA, plotting moduli as a function of temperature at a single frequency. The bold lines illustrate how the elastic modulus decreases at the transition, and the loss tangent displays a maximum. The plain line illustrates how the results would change if the experiment were done at a lower frequency, or if a plasticiser were added to the polymer. The lower plot shows typical results from an ultrasonics study, where the acoustic velocity decreases through the transition and the acoustic absorption displays a maximum.

constant. The velocity decreases as the temperature rises, undergoing a sigmoidal change in slope as the polymer undergoes the primary relaxation. A large peak in the acoustic absorption is associated with this relaxation, while smaller peaks at lower temperatures (not shown in Figure 3) would indicate $\beta$ and $\gamma$ relaxations. As described above with reference to DMA, lowering the frequency or introducing a plasticizer would shift the features of the curves to lower temperatures.

In this paper we explore the use of the FPW device to probe the transitions of polymer films applied to the device surface. Both the acoustic velocity (as measured by the frequency) and the acoustic attenuation (as indicated by the amplitude of the oscillator signal) are monitored; this approach is directly analogous to conventional ultrasonic methods. However, our experiments on polymer thin films differ from conventional methods of probing glass transitions, which make measurements on bulk materials. The polymer films on the FPW device surface are usually ca. 0.5 to 1 $\mu$m in thickness, which is much smaller than the acoustic wavelength (100 $\mu$m on our 5 MHz FPW devices) probing the sample.

The glass transition behaviors of polymer thin films have previously been investigated using SAW devices. Wohltjen and Dessy originally reported that the softening of polymer films could be observed on SAW devices by following signal amplitude (12). Subsequently, Groetsch and Dessy reported similar studies (34). More recently, Ballantine and Wohltjen attempted to observe the dynamic glass transition by following SAW device frequency (35). In a study following both SAW velocity and attenuation simultaneously, Martin and Frye have observed the dynamic relaxation of one component of a block copolymer, and examined the effects of vapor sorption on the relaxation process and the SAW sensor signals (36). These studies using SAW devices will be examined in more detail in the Discussion.

Our investigation of polymer films on FPW devices has three purposes. First, we wish to elucidate the properties and transition behaviors of amorphous polymers on planar acoustic devices. (The discussion of fundamental polymer physics above is an essential prerequisite to achieving this goal.) Second, we demonstrate that the FPW device is capable of sensing these transitions, and that the results obtained are analogous to those of conventional bulk-wave ultrasonic experiments. Third, the physical properties and transition behaviors of amorphous polymers on planar acoustic devices have important consequences for the use of polymer-coated FPW and SAW devices as vapor sensors, and these will be discussed.

## EXPERIMENTAL SECTION

**Materials.** Poly(vinyl acetate), secondary standard, was obtained from Aldrich: typical M.W. 194,800, typical M.N. 47,700. Poly(isobutylene), low molecular weight, was obtained from Aldrich: average M.W. 380,000, density 0.918, glass transition temperature -76°C. Poly(vinyl propionate) was obtained from Aldrich as a solution in toluene: polymer density 1.02, glass transition temperature 10°C. Poly(t-butyl acrylate) was obtained from Polysciences as a solution in toluene. Solutions in toluene were converted to the solid polymer by rotary evaporation and removal of residual toluene as the azeotrope with ethanol.

**FPW Devices.** The FPW devices were fabricated as described in references 7 and 8. The membranes consisted of a 2.0 μm silicon nitride layer, a 0.2 μm aluminum ground plane, and a 0.7 μm ZnO piezoelectric layer. The interdigital transducers were fabricated with 25 μm fingers and 25 μm spaces in between, giving a 100 μm wavelength. These devices operated at 5 MHz. All experiments except the initial experiments with poly(vinyl acetate) were carried out using 5 MHz devices. Initial experiments with poly(vinyl acetate) were done with a device having a 2.3 μm silicon nitride layer and 1 μm ZnO layer operating at 5.5 MHz. Each device was mounted in a small machined stainless steel chamber with four SMB coaxial feedthroughs. Gold wires were soldered to the contact pads of the FPW device and soldered to the feedthroughs. Feedthroughs were connected to a separate feedback amplifier circuit with RG174U cables and SMB fittings.The stainless steel chamber was fitted with a teflon lid equippedwith gas inlet and outlet tubes.

The FPW device was operated as the resonating element in the feedback amplifier circuit. The interdigital transducers were driven differentially relative to the ground plane. The circuit consists of a one-stage Motorola MC1733 differential video amplifier and a buffer amplifier. No matching circuit was used. Power (+/- 6 VDC) was supplied by a Micronta adjustable dual-tracking DC power supply.

**Polymer Film Application.** Spray-coated polymer films were applied to the FPW device using an airbrush supplied with compressed dry nitrogen and a dilute solution of the polymer (approximately 10 mg/mL) in HPLC-grade chloroform (Aldrich). The oscillator frequency was monitored during deposition; the frequency change observed provides a measure of the amount of material applied. To begin coating, the airbrush was placed several inches away from the device and spraying was initiated with the nozzle

directed away from the device. Then the spray was passed over the device several times, followed by a pause to observe the change in frequency. This process was repeated many times until the desired frequency change was obtained. Films causing 100 to 300 kHz frequency changes were applied. This method distributes the polymer evenly over the entire membrane surface.

Spray-coated films were examined by optical microscopy with a Nikon Optiphot M microscope using reflected light Nomarski differential interference contrast. Films were examined before and after experiments. Films on the FPW device causing in the range of 100 to 300 kHz of frequency change completely covered the membrane surface. Based on the mass sensitivities of these FPW devices, typically -2 Hz/ng/cm$^2$ (9), and polymer densities near 1 g/mL, the thickness of a film causing 100 kHz frequency drop is ca. 0.5 μm thick. Prior to beginning our experiments, polymer films were annealed at temperatures well above their glass transitions for at least several hours under flowing dry nitrogen.

Polymer thin films that wet and adhere to the membrane surface throughout the temperature range examined are required for the types of experiments described. Adhesion was not a problem with the polymers examined so long as the membrane surface was rigorously clean. Clean oxide surfaces have high surface energies. (The silicon nitride membrane actually has a silicon oxide surface.) Surfaces with organic contaminants have lower surface energies and are more difficult to wet. For example, in one case a poly(vinyl propionate) film broke up into isolated beads on the FPW membrane when it was heated above 70°C. This process was accompanied with substantial losses in signal amplitude. Cleaning with chloroform, re-coating, and re-heating simply reproduced this behavior. Then, after removing the polymer with chloroform, we cleaned the membrane surface with a mixture of sulfuric acid and hydrogen peroxide, also referred to as piranha solution. (CAUTION: This solution should only be prepared by knowledgeable individuals in small quantities and disposed of properly after use. It should never be stored in closed containers. ) The next film of poly(vinyl propionate) was quite stable regardless of temperature. After annealing at 70°C, the only visible difference in the film was that the film surface was very smooth and even, as opposed to the slight roughness of freshly sprayed films (visible under the microscope).

**Device temperature control.** The FPW device in its mounting chamber was placed on the bottom of a brass box suspended in a Neslab refrigerated circulating water bath with a programmable digital temperature controller. Foam insulation was placed over the mounting chamber. The oscillator circuitry was located outside the brass box. Dry nitrogen at 50 mL/min. (controlled by an electronic mass-flow controller) was routed through a four foot section of 1/8" OD 1/16" ID Ni tubing coiled in the water bath before being fed into the teflon cap on the mounting chamber. Temperatures were monitored with a Cole-Parmer Thermister Thermometer (Model N-08502-16) and a YSI 427 small surface probe placed on the outside of the FPW stainless steel mounting package.

When monitoring frequency we ramped the temperature at a rate of +/-10 °C/hour. Amplitude measurements were carried out at ramp rates of +/-20 °C/hour. Polymer behavior was repeatable regardless of the direction of temperature change or the number of previous ramping experiments.

**Data Collection.** Temperature data were collected from the thermister thermometer by a microcomputer equipped with an A/D converter interface board. Frequency measurements were made using a Phillips PM6674 frequency counter with TCXO, transferring the data to a microcomputer using the IEEE-488 bus. Frequency data were usually collected at 1 minute intervals. Signal amplitudes were measured using a LeCroy 9400 Digital Oscilloscope and recorded manually.

## RESULTS

When we began this study, we routinely monitored the frequencies of polymer-coated FPW devices in oscillator circuits. The devices were maintained at a single temperature for use as vapor sensors (9). To investigate FPW device responses to changes in polymer properties, we varied the temperature at slow constant rates, continuing to monitor oscillator frequency. Monitoring oscillator frequency is equivalent to monitoring acoustic velocity since the two are directly related. Our first experiments, described below, showed that the FPW device frequency is influenced by changes occurring at the polymer $T_g$. In subsequent experiments, where we wished to observe polymer relaxation processes, we monitored signal amplitude as well as frequency. Peaks in sound absorption in ultrasonic studies and DMA loss maxima are characteristic of polymer relaxations occurring at $T_\alpha$ (25-30). In control experiments with no polymer film on the FPW device, changes in frequency and amplitude were linear or nearly so over the temperature ranges investigated.

For this study we selected homogeneous amorphous polymers whose properties were already well described in the literature. Thus we could evaluate our results on FPW devices against polymer properties known to change in certain temperature ranges. Polymer $T_g$ values are available from a wide variety of sources, so the primary criterion for the observation of $T_g$ was that it occur well within the temperature range of our experiments. (For example, polymer $T_g$ values can be found in catalogs, in compilations such as those in references 21-23, and in the primary literature.) The temperature of the primary relaxation, $T_\alpha$, varies with frequency, so we selected polymers whose relaxation behavior had been investigated at frequencies near our FPW device frequency. This information was obtained from literature describing the results of bulk-wave ultrasonic measurements and DMA.

Finally, it is useful to mention the differing effects of elastic modulus and viscosity on sensor frequencies before examining the results in detail. (When discussing planar acoustic sensors, the modulus referred to is always the shear modulus.) The sensitivities of the FPW device to these properties in thick gels have been modelled theoretically (1). A decrease in modulus causes frequency to decrease. A decrease in viscosity causes frequency to increase. Preliminary models for thin polymer films of 1 μm thickness on the FPW membrane indicate that decreases in frequency will again be observed when the elastic modulus decreases. We do not yet have a complete model for the dependence of FPW frequency on thin film viscosity changes, but we assume that decreases in viscosity will cause increases in frequency as they do when thick gels are used. These trends in

FPW frequency with changes in polymer viscoelastic properties are the same as those observed using polymer-coated SAW devices. Decreasing polymer modulus decreases the SAW frequency, as is well-known (13). SAW frequency increases due to polymer film viscosity decreases have recently been reported by Martin and Frye (36).

**The Static Glass Transition.** Poly(vinyl acetate) was selected for our first experiments because its $T_g$ is conveniently located just above room temperature at ca. 30°C (21,27,37). Following the frequency of a poly(vinyl acetate)-coated device as a function of temperature, we obtained the results shown in Figure 4. The data are linear above and below the transition, with a change in slope occurring at the transition temperature. This change, occuring from 33-38°C, is particularly evident in the derivative of the frequency-temperature plot, as shown in the lower plot of Figure 4. The temperature of the polymer-coated FPW device was ramped up and down many times, and the same results were always obtained. The change in slope is slightly sharper when the temperature is ramped up.

We also investigated poly(t-butyl acrylate), whose $T_g$ occurs at ca. 43°C (23,38,39). The results are shown in Figure 5. Again, the frequency-temperature plot is linear below and above $T_g$ with a change in slope at $T_g$. From the graph showing the slope of the temperature-frequency plot, we see that the transition is in the range of 40-44°C, in good agreement with the literature value of $T_g$.

*The above results demonstrate that the FPW device is sensitive to those frequency-independent properties of polymers that change at $T_g$, and that this change can be observed by following acoustic velocity via the device frequency.* The direction of the change in FPW frequency is consistent with the decrease in modulus occurring as the free volume of the polymer expands above $T_g$. Our results are similar to those of dilatometric and ultrasonic studies as they were illustrated in Figure 2.

Since the behavior we observe must be related to the change in coefficient of thermal expansion at $T_g$, we compared the slopes from our plots with published coefficients of thermal expansion. The rate of change of frequency with temperature of the bare 5.5 MHz FPW device used for the poly(vinyl acetate) experiments above was -260Hz/°C. With the poly(vinyl acetate) film applied, values of -1070 Hz/°C and -540 Hz/°C were obtained above and below the glass transition, respectively. By subtraction, values of -810 and -280 Hz/°C above and below the transition are attributable to the

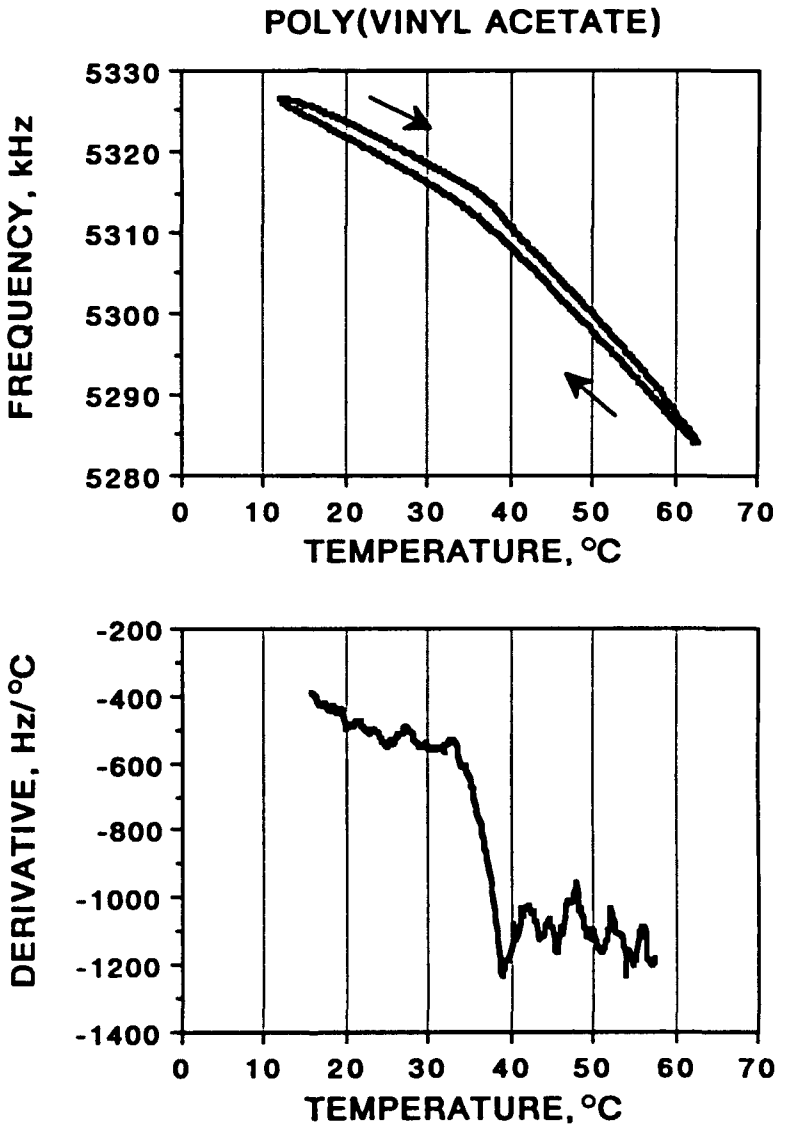


Figure 4. The effect of temperature on the frequency of a poly(vinyl acetate)-coated FPW device, showing the glass transition of the poly(vinyl acetate). The lower plot shows the derivative of the top trace in the upper plot, where the device frequency is being monitored as the temperature is ramped up.

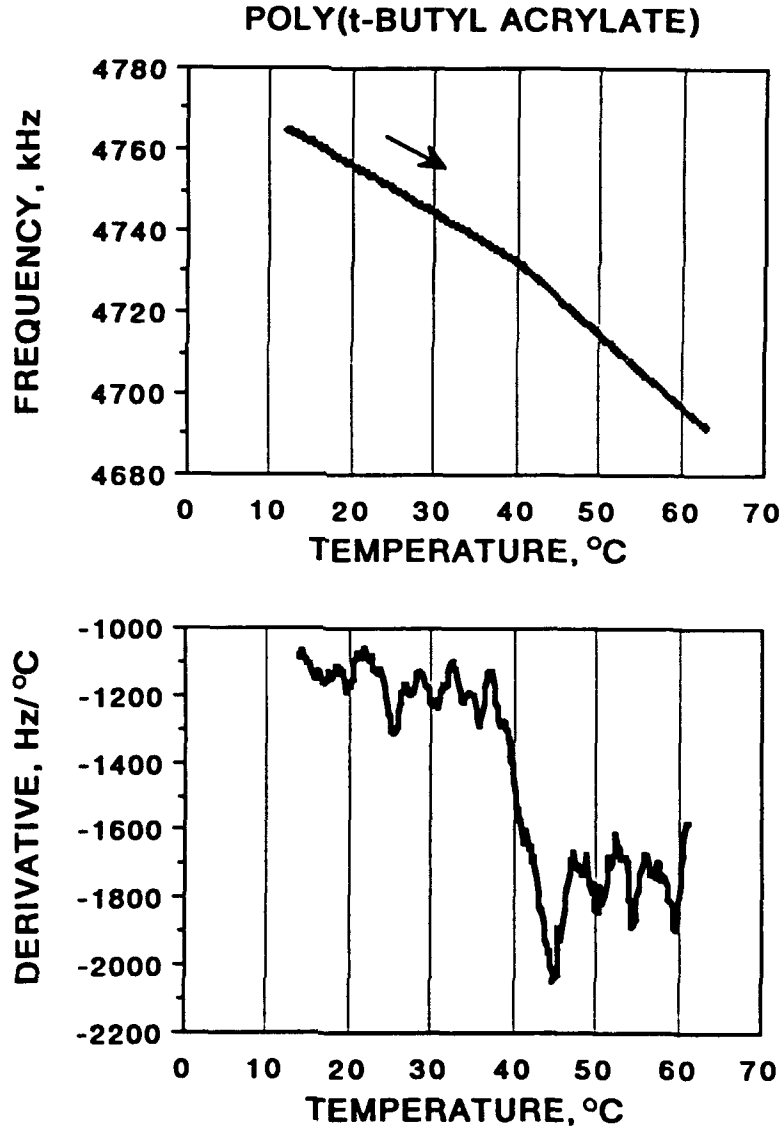


Figure 5. The effect of temperature on the frequency of a poly(t-butyl acrylate)-coated FPW device, showing the glass transition of the poly(t-butyl acrylate). In this case the traces for ramping the temperature up and down were superimposable; the data for ramping the temperature up are shown. The lower plot shows the derivative of the trace in the upper plot.

polymer. These results were initially intriguing because the ratio of these values (2.9:1) is close to the ratio of thermal expansion coefficients for poly(vinyl acetate) above and below the $T_g$ (2.6:1 or 2.9:1, depending on the source of the data) (21). However, in a subsequent experiment with poly(vinyl acetate) on a 5.0 MHz FPW device, a ratio of only 2.3:1 was obtained.

The rate of change of frequency with temperature of the 5.0 MHz device used in the poly(t-butyl acrylate) experiment was -640 Hz/°C. With the poly(t-butyl acrylate) film applied, values of -1750 Hz/°C above the transition and -1170 Hz/°C below the transition were observed, giving values of -1110 and -530 Hz/°C attributable to the polymer. The ratio of these values is ca. 2:1, while the ratio of thermal expansion coefficients for this polymer is reported to be nearly 4:1 (21). (The high ratio of thermal expansion coefficients reported for this polymer in reference 21 was the reason we selected it for investigation.) Although the ratio of 4:1 reported for this polymer is open to some doubt because the reference trail leads back only to a private communication (40), we accept it here for the time being. We then conclude that we cannot use the slopes of our FPW frequency-temperature plots to predict ratios of polymer thermal expansion coefficients. The device must sense some property that is a function of the thermal expansion of the polymer, most likely the modulus.

**Polymer Relaxation Processes.** Studies of polymer relaxation were carried out over a larger temperature range than the experiments above. Both the frequency and the amplitude of the FPW oscillator signal were monitored. The signal observed when the 5.0 FPW device membrane was bare (i.e., without a polymer thin film applied) was 425 mV at room temperature. The amplitude decreased with increasing temperature at a rate of just under 5 mV per 10°C. Significantly greater variations in the signal amplitude with temperature were observed when polymer films were present on the membrane. These amplitude changes are proportional to the attenuation of the acoustic energy by the polymer material (i.e., decreases in signal amplitude indicate increases in attenuation).

Over the temperature range of -20 to 100°C, changes in the frequency of the 5.0 MHz device used were essentially linear up to 50 or 60°C. The rate of frequency change deviated slightly (concave upward) at higher temperatures. The data were fitted with a second-order polynomial expression, giving $y = 4986.5 - 0.60073x + 5.8326 \times 10^{-4} x^2$, $R^2 = 1.000$, where y is frequency in kHz and x is temperature in °C. The frequency of the device as a function of temperature is shown graphically in Figure 6.

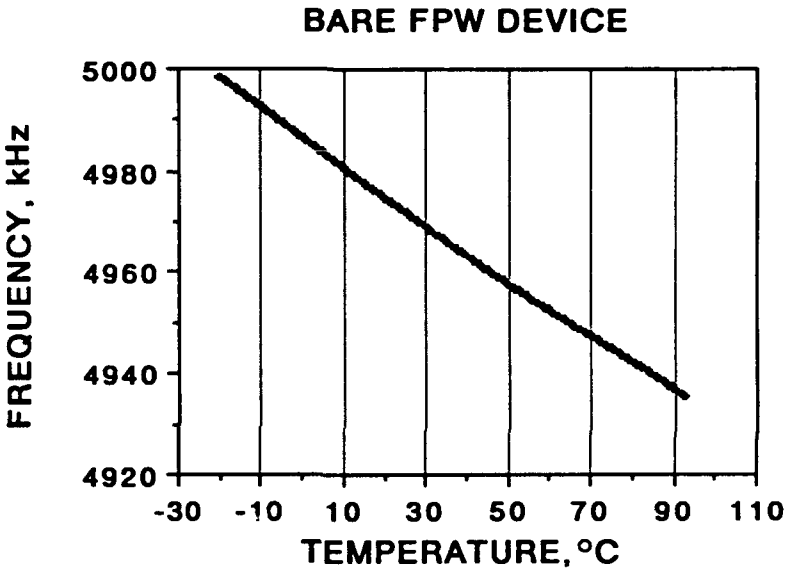


Figure 6. The effect of temperature on the frequency of a bare 5.0 MHz FPW device over the -20 to 100°C temperature range.

We selected poly(isobutylene) for our first efforts to observe polymer relaxation processes on the basis of a previous paper by Ivey et al. describing ultrasonic studies at various frequencies, including 3 MHz and 10 MHz (41). This paper shows plots of both sound velocity and sound absorption in a cured sample of butyl rubber. Broad peaks of sound absorption with maxima at ca. 25°C at 3 MHz and 40°C at 10 MHz indicate the occurence of the $\alpha$ relaxation. Sound velocity curves in the same temperature region are non-linear. Butyl rubber is actually a copolymer of isobutylene with a few percent of isoprene (28). Results obtained with this rubber may not be identical to those of a pure uncross-linked poly(isobutylene), but they are representative of the type of behavior to be expected. The viscoelastic behavior of poly(isobutylene) is described by McCrum et al. (27). A plot of $T_\alpha$ as a function of temperature and frequency in this reference suggests that the temperature of the $\alpha$ relaxation in the 1 to 10 MHz frequency domain should be in between 0 to 20°C. The $T_g$ of poly(isobutylene) is -76°C.

Our first indication that poly(isobutylene) caused a peak in the attenuation of the FPW signal amplitude came when we applied a coating causing 260 kHz of frequency decrease. Although this amount of coating is normally not a problem, the oscillation of the poly(isobutylene)-coated device at room temperature was erratic. At higher temperatures, however, the oscillation was quite stable. When the temperature was decreased from 75°C to 5°C, the oscillation stopped at 24°C. When the temperature was rapidly raised, oscillation resumed at ca. 30°C. These results indicated that the signal attenuation was decreasing above 30°C, and suggested that a sound absorption peak might be present below 30°C.

We then investigated a device coated with only 113 kHz of poly(isobutylene) so that oscillation could be sustained through a wider temperature range. The device was ramped from -20 to 100°C repeatedly. Our frequency and amplitude results are shown in Figure 7. The frequency data shown are the difference between the frequency of the poly(isobutylene)-coated device and the bare device. Thus, the inherent device temperature drift and its slight curvature at high temperatures have been subtracted out. The frequency value at 25°C indicates the amount of polymer coating on the device in kHz and is in agreement with the amount measured at room temperature when the film was applied.

The frequency-temperature plot is highly curved (concave upward). It is very similar in appearance to the sound velocity curves published by Ivey et al. where the slope changes in a sigmoidal fashion. The FPW frequency results also appear to be sigmoidal in shape, although more data at lower temperatures would be required to fully confirm this.

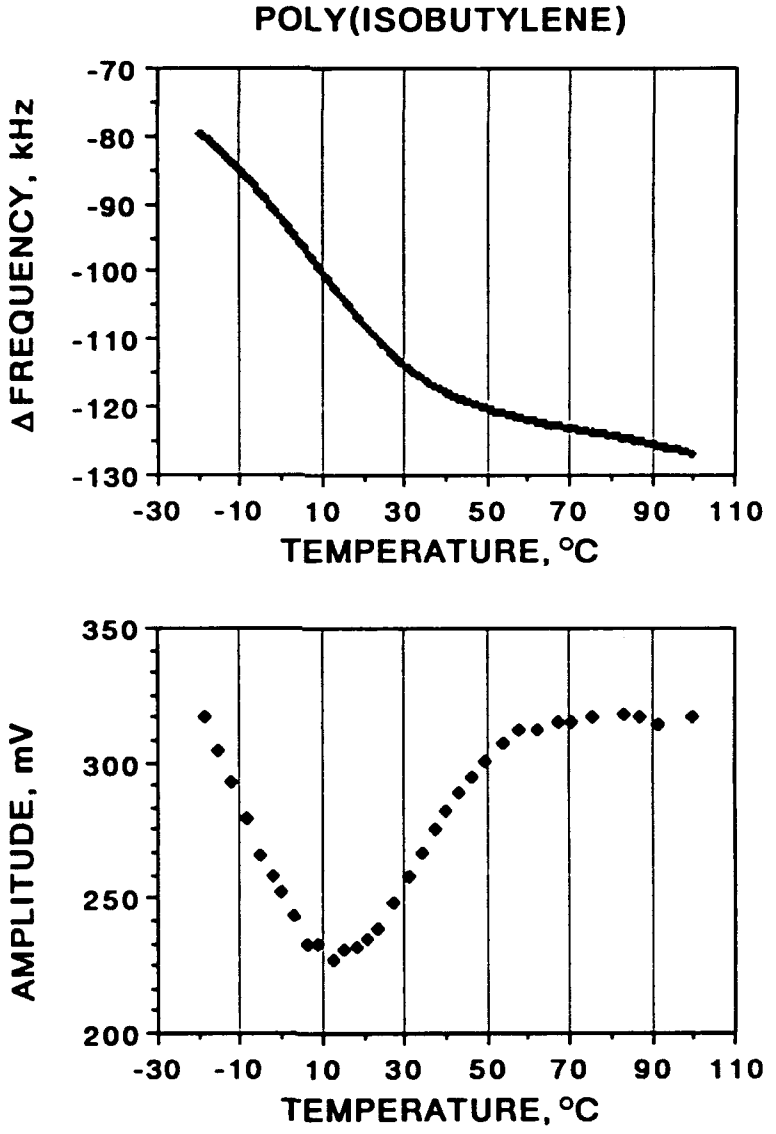


Figure 7. The effect of temperature on the frequency (upper plot) and amplitude (lower plot) of a poly(isobutylene)-coated FPW device, showing the primary relaxation at 15°C.

The plot of the signal amplitude clearly shows a broad minimum, indicating a maximum in signal attenuation around 15°C which is associated with the sigmoidal changes in frequency. We observe the maximum at slightly lower temperatures than Ivey et al., but consistent with the compilation in reference 27. The overall behavior we observed is clearly in accord with the known properties of this polymer. Therefore, we assign these FPW signal characteristics around 15°C to the $\alpha$ relaxation.

We also investigated poly(vinyl propionate). For comparison, the viscoelastic behavior of this polymer is described by McCrum et al. (27), and plots of longitudinal sound velocity and absorption at 2 MHz are shown in a paper by Thurn and Wolf (42). The latter authors observed a peak in sound absorption at 54°C and a corresponding sigmoidal change in sound velocity. The $T_g$ of this polymer is ca. 10°C. Our frequency and amplitude results on the FPW device are shown in Figure 8. A peak in signal attenuation is observed at 70°C. In addition, there is a corresponding sigmoidal change in the frequency-temperature plot. These results agree very well in form, though not precisely in temperature, with the results of Thurn and Wolf, and thus indicate the $\alpha$ relaxation.

There are also changes in the FPW device frequency-temperature plot at lower temperatures near $T_g$ . They are not particularly dramatic, however, and the $T_g$ is not as clearly indicated as it had been in the poly(vinyl acetate) and poly(t-butyl acrylate) experiments. Changes in slope are seen at ca. 5°C and again at ca. -5°C. Our results, however, are consistent with those of Thurn and Wolf, who also do not see clear changes of the sound velocity at the $T_g$ of this polymer. The results suggest two possibilities. First, it may be that the property sensed by the FPW device does not undergo a large change as this polymer traverses the $T_g$. Second, it is possible that a $\beta$ relaxation process is occurring in the same temperature region and its effects on FPW device frequency obscure the $T_g$ effect. Indeed, the FPW device amplitude plot suggests a small shoulder that would be consistent with such a relaxation. However, the shoulder is near the limit of our precision in measuring amplitude. Repeat experiments collecting amplitude data at more frequent intervals failed to confirm or deny the presence of this shoulder. Thurn and Wolf, however, do report small peaks or shoulders in their sound absorption plot at 15, -5, and -28°C which may indicate secondary relaxations.

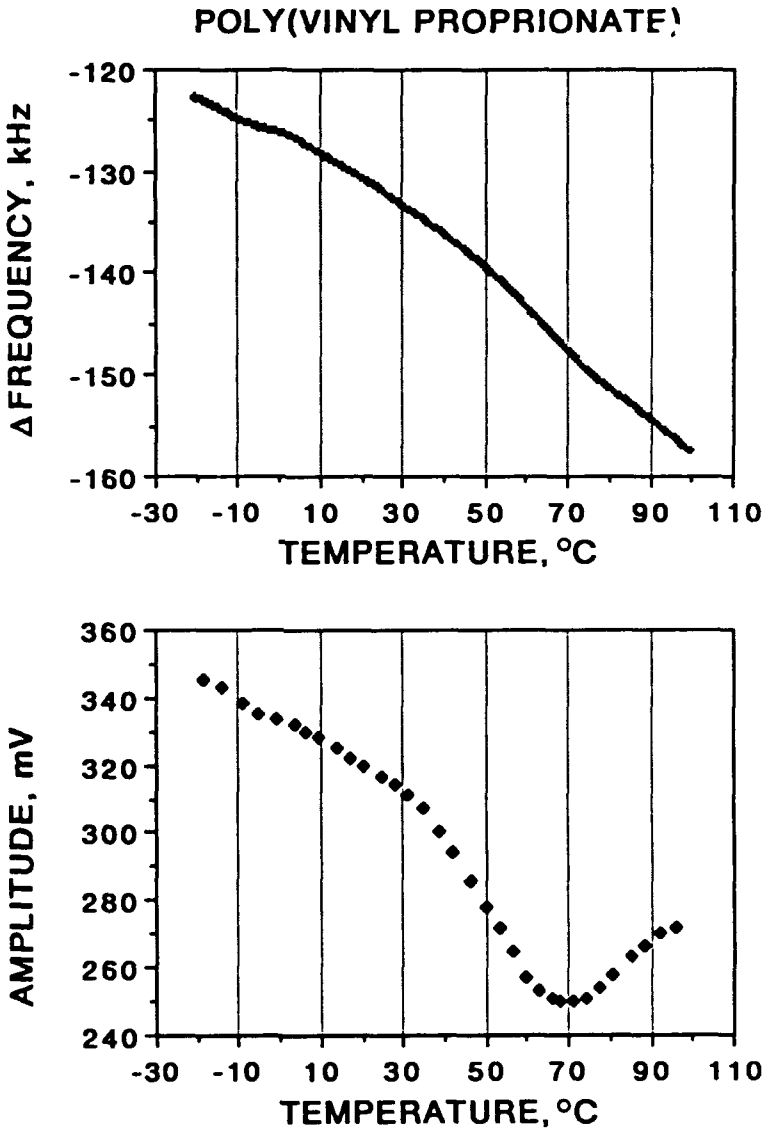


Figure 8. The effect of temperature on the frequency (upper plot) and amplitude (lower plot) of a poly(vinyl propionate)-coated FPW device, showing the primary relaxation at 70°C.

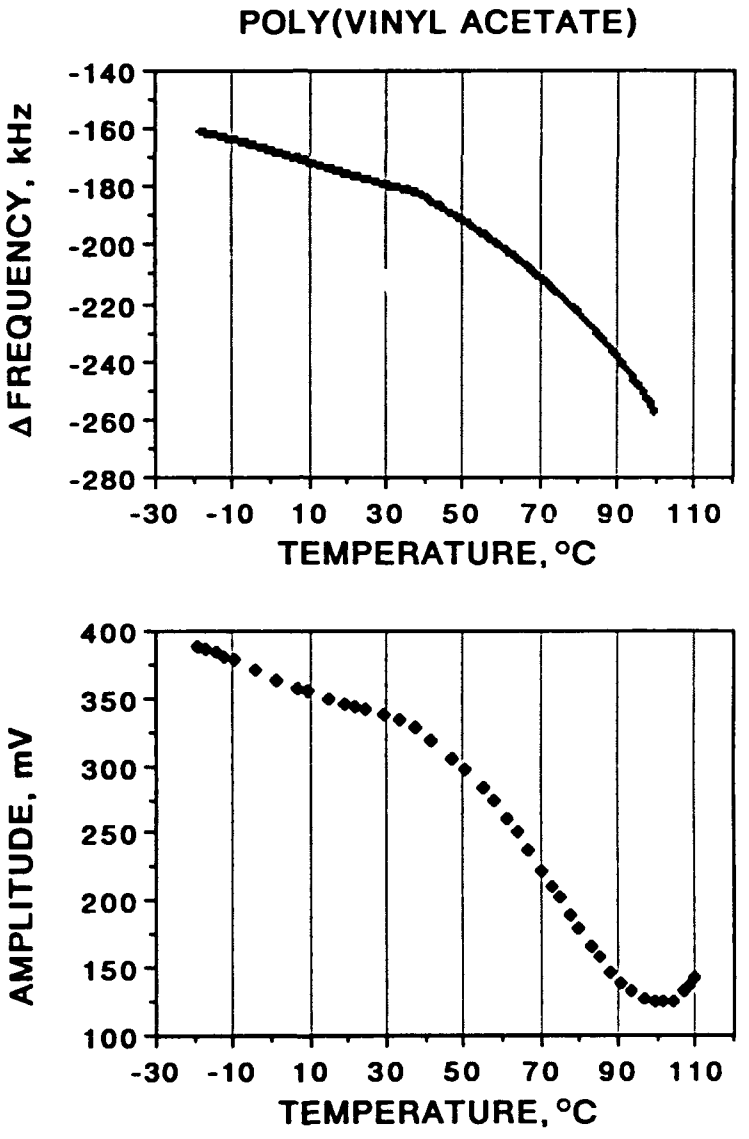


Figure 9. The effect of temperature on the frequency (upper plot) and amplitude (lower plot) of a poly(vinyl acetate)-coated FPW device, showing the primary relaxation at 100°C, and the static glass transition between 30 and 40°C.

Finally, we reexamined poly(vinyl acetate) over a larger temperature range. Data compiled by McCrum et al. in a plot of $T_\alpha$ as a function of temperature and frequency indicate $T_\alpha$ falls between 90 to 120 °C in the 1 to 10 MHz range (27). Thurn and Wolf show plots of sound velocity and absorption at 2 MHz with a loss peak at 93°C (42). A report by Nolle and Mowry on ultrasonic studies of Vinylite indicates that $T_\alpha$ is above 90°C at a frequency of 10 MHz (43). (Vinylite is a tradename for poly(vinyl acetate) formulations.) Our frequency and amplitude results for poly(vinyl acetate) on the FPW device, shown in Figure 9, indicate that a signal attenuation maximum occurs at 100°C. The frequency curves downward as the temperature approaches 100°C. These results are very similar in appearance to the plots shown by Thurn and Wolf. The FPW frequency plot also shows the $T_g$ as a clear discontinuity in slope between 30 and 40°C, as observed previously. We thought we might observe a $\beta$ relaxation, but we found no definitive evidence for such a transition in either the frequency or amplitude plot. This could mean that the FPW device is not sensitive to this transition in this polymer, or that the transition is not occurring in our experimental temperature range. Thurn and Wolf report a $\beta$ relaxation in their poly(vinyl acetate) sample at -10°C at 2 MHz.

To summarize, the results above for three separate polymers demonstrate unambiguously that the temperature of the $\alpha$ relaxation of a polymer applied as a thin film on the FPW device is shifted to temperatures higher than the $T_g$. The flexural Lamb waves are therefore coupled into the polymer film and strain the polymer. The frequency and amplitude behaviors observed, and the positions of the $\alpha$ relaxations at the FPW device frequency, are entirely consistent with the results obtained by independent methods such as bulk-wave ultrasonic studies. Large peaks in FPW signal attenuation are characteristic of the $\alpha$ relaxation process, with corresponding sigmoidal changes in acoustic velocity. The direction of the sigmoidal changes in FPW acoustic velocity correspond to the effect of decreasing modulus, and are in the same direction as the sigmoidal changes of sound velocity in ultrasonic studies on bulk polymer samples. The results with poly(vinyl acetate) graphically demonstrate that separate transitions occur at both $T_g$ and $T_\alpha$ in polymer films applied to the FPW device.

## DISCUSSION

The use of planar acoustic devices to detect transitions in polymer samples was first reported by Wohltjen and Dessy (12). These investigators used 30 MHz SAW devices and monitored signal amplitude. Polymers such as poly(ethylene terephthalate), polycarbonate, and polysulfone were investigated as thin samples pressed against the SAW device surface. Raising the temperature caused a sharp drop in amplitude when the static $T_g$ of the sample was reached. This effect was not reversible. These results were explained by noting that microscopic roughness limits contact between the glassy polymer film and the SAW device surface when the experiment is assembled. Consequently, the surface waves are not efficiently coupled into the polymer material at the beginning of the experiment. When the polymer softens at the $T_g$, it is pressed into more intimate contact with the SAW surface and acoustic losses into the polymer increase. Each result obtained by this method was in agreement with the known static $T_g$ of the polymer and with DMA at a low frequency (3.5 Hz).

Wohltjen and Dessy investigated a single polymer, poly(methyl methacrylate), as a film cast directly on the device surface. In this case, intimate contact between the polymer film and the SAW surface should exist throughout the experiment. A reversible drop in signal amplitude was observed at 150°C, which is above the static $T_g$ of this polymer at ca. 105°C. This result was interpreted as indicating that the surface waves were coupled into the polymer film, inducing periodic strains in the polymer, and increasing the temperature of the transition according to the time-temperature superposition principle. While the physical observation is undoubtedly correct and the interpretation is reasonable, it is troublesome that the results are inconsistent with the known properties of poly(methyl methacrylate). This polymer has been widely studied by ultrasonic methods and the $\alpha$ relaxation occurs at temperatures above 200°C at frequencies above 1 MHz (44). We can only speculate that the polymer sample in the SAW investigation may have contained some plasticizer, which would have lowered the relaxation temperature.

Investigations of polymer samples on 30 MHz SAW devices were continued by Groetsch and Dessy (34). Again, both cast and pressed films were examined, and signal amplitude was measured. Polystyrene, polysulfone, poly(methyl methacrylate), and polycarbonate were examined as cast films. Results on SAW devices were compared with $T_g$ values determined by DSC and loss peaks observed by DMA at 1 Hz. These authors defined two temperatures of interest from the SAW amplitude-temperature profiles. The first, referred to as a "knee", was the onset of decreases in amplitude. The second was the temperature of a subsequent minimum in the amplitude profile. The temperatures of the

SAW knees were quite close to the $T_g$ values determined by DSC. With one exception, poly(methyl methacrylate), the temperatures of the SAW amplitude minima were similar to the loss peaks observed by DMA at 1 Hz. These results are difficult to reconcile with the hypothesis that the high frequency surface waves couple into the polymer films, stress the polymer, and increase dynamic transition temperatures. If this were the case, then one would expect transition temperatures at 30 MHz on the SAW device to be significantly higher than those determined at only 1 Hz by DMA.

The temperatures of the SAW minima for poly(methyl methacrylate) and polystyrene are also not consistent with known dynamic relaxation behavior of these polymers at high frequencies. The poly(methyl methacrylate) results were similar to those reported previously by Wohltjen. The position of the polystyrene SAW minimum reported at 110°C is much lower than the temperatures of the known transitions of polystyrene at high frequencies: at frequencies above 1 MHz, the $\alpha$ relaxation of this polymer occurs at temperatures above 150°C (27); and recent bulk-wave ultrasonic studies indicate transition temperatures of 154 and 163°C for polystyrene samples at 1.75 MHz (45). The differences between the SAW results and the known properties of polystyrene at high frequencies suggest that either the surface waves do not induce strains in the polymer that cause relaxation temperatures to rise, or that the SAW minimum observed is due to some process other than the $\alpha$ relaxation. However, the observed minimum cannot be explained by the $\beta$ relaxation for polystyrene either, since this relaxation is also expected to occur well above 110°C at 30 MHz (27). The bulk of the evidence in the paper by Groetsch and Dessy is not consistent with the hypothesis that surface waves stress cast polymer films and raise transition temperatures, nor do the authors suggest that such effects occur.

In a later study, Ballantine and Wohltjen attempted to demonstrate that SAW oscillator frequencies (as opposed to the amplitude experiments described above) of polymer-coated 158 MHz SAW devices could be used to detect polymer glass transitions (35). It was assumed that the frequency of the SAW would raise polymer transition temperatures. The experiments did not investigate whether SAW frequency changes would occur in the range of the static $T_g$. Of the four polymers examined, three were examined only at temperatures well above their static $T_g$, while a fourth was examined at temperatures beginning quite near the $T_g$.

The results of these SAW frequency investigations were difficult to interpret fully. At the time a complete model to predict how changes in polymer viscoelastic properties would influence SAW frequencies had not been developed. A model including elastic effects was presented, but it is now known that viscous effects can be significant. Nor were the actual dynamic transition temperatures of the selected polymers known at high

frequencies (as determined by independent methods such as DMA or bulk-wave ultrasonic studies). Fluoropolyol showed no dramatic features in the frequency-temperature profile. Poly(ethylene maleate) caused a frequency minimum, but its significance is unclear in the absence of corresponding amplitude measurements, independent knowledge of this polymer's transition behavior at high frequencies, or a theoretical viscoelastic model for comparison. Poly(caprolactone) displayed interesting behavior at its melting temperature, but no clear indication of a dynamic transition is apparent. Ethyl cellulose, whose $T_g$ is 43°C, caused a sigmoidal change in the frequency in the 95 to 110°C temperature range. Up to about 95°C the frequency decreased, apparently as a result of thermal expansion . (This statement is in reference to the frequency of the individual coated delay line. The difference frequency between the coated and the bare delay line of the dual delay line device is increasing.) Then the slope of the frequency-temperature plot reversed direction and frequencies increased up to ca. 110°C, after which they decreased again. Since both conventional bulk-wave ultrasonic studies and our FPW device results show sigmoidal changes in acoustic velocity at $T_\alpha$, these results could be an indication of a frequency-dependent relaxation process occurring well above $T_g$. (However, the acoustic velocities are increasing through this potential relaxation process on the SAW device, whereas velocities decrease through the relaxation processes demonstrated in bulk-wave ultrasonic studies and FPW experiments. We shall return to this point below.) A definitive assignment of these changes in frequency to a relaxation would require corresponding SAW attenuation measurements and/or independent knowledge of the relaxation behavior of ethyl cellulose at the SAW frequency.

Recently, Martin and Frye published an investigation of a polymer-coated 97 MHz SAW device where they monitored both SAW velocity and attenuation simultaneously (36). Data collected between 12 and 78°C using a cast film of styrene-butadiene-styrene triblock copolymer were compared with a theoretical Maxwell model for polymer viscoelasticity. They obtained an excellent fit between their data and their model indicating a viscoelastic relaxation process at a temperature of 53°C. The signal attenuation peaks and the SAW velocity increases as the relaxation occurs. Block copolymers of this sort actually have separate transitions associated with discrete domains of each component (20,44). Since the $T_g$ of polystyrene and its $\alpha$ and $\beta$ relaxations at 97 MHz are all above the experimental temperature range (27), the dynamic transition observed at 53°C is most likely due to a relaxation in the poly(butadiene). For comparison, the static $T_g$ of poly(butadiene) is only ca. -95°C. This study including velocity measurements, attenuation measurements, and a theoretical model for viscoelasticity provides convincing evidence that surface waves

can couple into thin polymer films and raise dynamic transition temperatures, as originally proposed by Wohltjen and Dessy (12).

Our experimental results on the FPW device are the first to demonstrate that polymer transitions can be observed on a planar acoustic device at both the static $T_g$ and dynamic $T_\alpha$. This result is particularly clear with poly(vinyl acetate). No previous SAW paper had indicated that changes should or could be seen at both these temperatures under dynamic conditions. Moreover, our results are correlated with known properties of the polymers investigated and closely parallel acoustic velocity and absorption behavior in conventional ultrasonic studies. The results we report show unambiguously that flexural Lamb waves couple into applied polymer overlayers, causing a periodic strain in the polymer which shifts $T_\alpha$ to temperatures well above $T_g$.

It is interesting to compare the changes in acoustic velocity (or frequency) associated with relaxations observed by ultrasonic methods, FPW device experiments, and SAW device experiments. The velocity *decreases* through the $\alpha$ relaxation (as temperature is increased) in bulk-wave ultrasonic and FPW device experiments. The direction of the response on the FPW device appears to be dominated by the decreases in modulus associated with the relaxation. By contrast, on the SAW device coated with styrene-butadiene-styrene triblock copolymer, acoustic velocities *increased* through the relaxation process, indicating that viscosity effects dominated in this case. Acoustic velocity *increases* were also observed with ethyl cellulose on a SAW device within a limited temperature range, possibly due to a relaxation process. If one were to generalize (or overgeneralize) from these examples, one would conclude that modulus effects dominate on FPW devices, while viscosity effects dominate on SAW devices, giving rise to responses in opposite directions.

Nevertheless, we hasten to point out that both styrene-butadiene-styrene triblock copolymer and ethyl cellulose are heterogeneous materials, with hard domains interspersed with soft amorphous domains. In the copolymer, the polystyrene domains are hard; in the ethyl cellulose, hard crystalline domains exist (melting temperature 165°C). It is therefore not clear whether the differences between the SAW results with the heterogeneous polymers and our FPW results with homogeneous amorphous polymers are due to the types of acoustic waves, the device frequencies, the polymer morphologies, or some combination of these factors. It is also not clear whether the SAW results cited above can be generalized to other polymer-coated SAW devices. (SAW studies using homogeneous polymers of known transition behavior at high frequencies would help to clarify these points.)

We can find some justification for a hypothesis that increasing the frequency from 5 MHz on a FPW device to 100 MHz or more on a SAW device might contribute to differences in response behavior, though we wish to emphasize that we are not implying that this is the only factor, nor do we know how significant it might be. As stated succinctly by Ferry in his classic treatment of polymer viscoelasticity, the stress in a perfectly elastic solid is proportional to the strain but independent of the rate of strain (26). For a perfectly viscous liquid, the stress is proportional to the rate of strain, but independent of the strain itself. Viscoelastic polymers have both liquid and solid characteristics. The complex shear modulus is expressed as a combination of real and imaginary terms, where the real term involves the elastic (or storage) modulus, and is *frequency-independent*. The imaginary term involves viscosity and is *frequency-dependent*. As frequencies increase, the magnitude of the imaginary term containing the viscosity increases relative to the real term containing the elastic modulus.

An understanding of polymer transitions on planar acoustic devices has significant implications for the use of polymer films on acoustic vapor sensors. First, it is clear that the polymer films contribute significantly to the temperature drift of such sensors. This point is applicable to both FPW and SAW sensors. No effort has been made thus far to reduce the inherent temperature drift of FPW devices, although a number of approaches could be taken to achieve this. However, if a completely temperature-stable device were fabricated, the application of a polymer film would create temperature drift because polymer properties sensed by the device vary with temperature. Therefore, efforts to reduce inherent temperature drift of the acoustic devices may not be worthwhile for ultrasonic sensors that employ sorbent polymers.

Second, in vapor sensor applications, it is useful to select a polymer whose $T_g$ is below the operating temperature of the sensor. Diffusion of organic vapors into glassy polymers below $T_g$ can be quite slow. Diffusion is much more rapid above the $T_g$ where the free volume is greater. Consequently, the response time of a polymer-coated sensor will be faster above Tg (if response times are diffusion limited). This criterion for sorbent polymer selection is applicable even under dynamic conditions. The increases in free volume begin to occur at $T_g$, regardless of sensor frequency. Our results on the FPW device showing changes in the slopes of frequency-temperature plots at $T_g$ provide clear experimental evidence that polymer properties do indeed change at the static $T_g$ under dynamic operating conditions.

Third, when a thin non-conducting isotropic thin film is applied to the surface of a SAW device, both gravimetric and elastic effects may influence the frequency shift observed (13). If the film is soft with an elastic modulus of ca. $10^7$ dynes/cm$^2$, a value

typical of amorphous polymers above their $T_g$ under static conditions, elastic effects are completely negligible compared to gravimetric effects. For a harder film having an elastic modulus of ca. $10^{10}$ dynes/cm$^2$, a value typical of glassy polymers below their Tg, elastic effects will be 10-15% as large as gravimetric effects and of opposite sign. (These approximations assume a SAW device on ST-cut quartz and a polymer density near 1 g/mL.) If an amorphous polymer is applied at a temperature above its $T_g$ and below its $T_\alpha$, an interesting situation arises. Assuming that the surface waves do couple into the film and raise $T_\alpha$ to a temperature above $T_g$, then the material appears to be stiff to the high-frequency waves that are probing the material. However, the polymer will probably not appear to be quite as stiff as a glassy polymer below $T_g$: the modulus is also affected by the polymer free volume, and the free volume of this polymer is greater than that of a glassy polymer. We emphasize that so long as the strains are small and the polymer behavior is in the linear viscoelastic regime, the waves do not actually change the state of the polymer. The material has not actually been stiffened by the high frequency periodic strains. If it were probed simultaneously be a low frequency method, then one would obtain the modulus characteristic of the material at the lower frequency. (This argument follows from the Boltzman superposition principle (25,26).)

Fourth, the occurrence of frequency changes in response to relaxation processes has consequences for vapor sensors if the polymer-coated sensor is operated at a temperature between $T_g$ and $T_\alpha$. The usual effect of vapor sorption is to decrease its frequency, and we will refer to a response in this direction as a "normal" response. This is the type of response expected from mass-loading, although it is possible that reductions in modulus that could occur on vapor sorption also contribute to responses in this direction. In addition to the normal response, the vapor will also plasticize the polymer and reduce the temperature of the primary relaxation, $T_\alpha$. In the arguments below, we will consider two cases. In one case, relaxation causes sigmoidal decreases in frequency, as demonstrated above for polymer-coated FPW devices operating at 5.0 MHz. In the second case, we consider the consequences if relaxation processes cause sigmoidal increases in frequency. This case could be a high frequency SAW device with a coating such as styrene-butadiene-styrene triblock copolymer. Of course, a third case also exists: relaxation processes could occur without any effect on frequency. Following the arguments presented above, it is possible that in some cases, the opposing effects of modulus and viscosity decreases on frequency could cancel one another out. Then relaxation processes would not play a role in vapor sensor response, even though they might be occuring.

In Figure 10 we present a hypothetical illustration of the frequency-temperature plot of a polymer-coated acoustic device at temperatures starting above $T_g$ and increasing to above $T_\alpha$. In this case, the relaxation at $T_\alpha$ causes sigmoidal decreases in frequency. We select temperatures above $T_g$ to promote diffusion as discussed above. The upper bold line shows the sensor frequencies in the absence of vapor. The lower plain line shows the hypothetical frequency-temperature plot for the same sensor exposed to a fixed concentration of vapor throughout the experiment. Three principles were used to construct this line. First, the normal response to vapor sorption decreases the oscillator frequency at any given temperature. Second, vapor sorption decreases as the temperature rises, so the normal response also decreases with temperature (i.e. the frequency difference between the bold and plain lines decreases with temperature). Third, $T_\alpha$ shifts to a lower temperature and is broadened because the sorbed vapor plasticizes the polymer. If the experiment were re-run at a higher vapor concentration, the line would shift further down and the relaxation would shift further to the left. In Figure 10, the effect of the relaxation has been exaggerated and the influence of temperature on sorption has been underestimated in order to more easily illustrate sensor behavior and relaxation effects over a large temperature range.

During isothermal operation as a vapor sensor, the response at temperature $T_1$ is entirely normal. At $T_2$ the response is normal and of lesser magnitude than the response at $T_1$. At $T_3$, however, the response is in the normal direction, but its magnitude is enhanced by the plasticizing effect of the sorbed vapor.

Now consider a series of experiments where the temperature is kept constant, and sensor responses are measured as the vapor concentration is varied to generate a calibration curve. Hypothetical calibration curves, based on the principles illustrated in Figure 10, are shown in Figure 11. We assume that the sorption isotherm of the vapor in the polymer is linear. When the sensor is operated at $T_1$, the calibration curve is linear. In this case, the sorbed vapor at its highest concentration is not sufficient to shift $T_\alpha$ all the way down to $T_1$. By contrast, at $T_3$, the normal response is immediately enhanced by the relaxation response. At higher concentrations (still at $T_3$), the response increases only by the additional normal response, resulting in the curved calibration line shown. At intermediate temperature $T_2$, the response is normal at low concentrations, until vapor concentrations are sufficient to shift $T_\alpha$ down to $T_2$. Then the responses are enhanced by the relaxation.

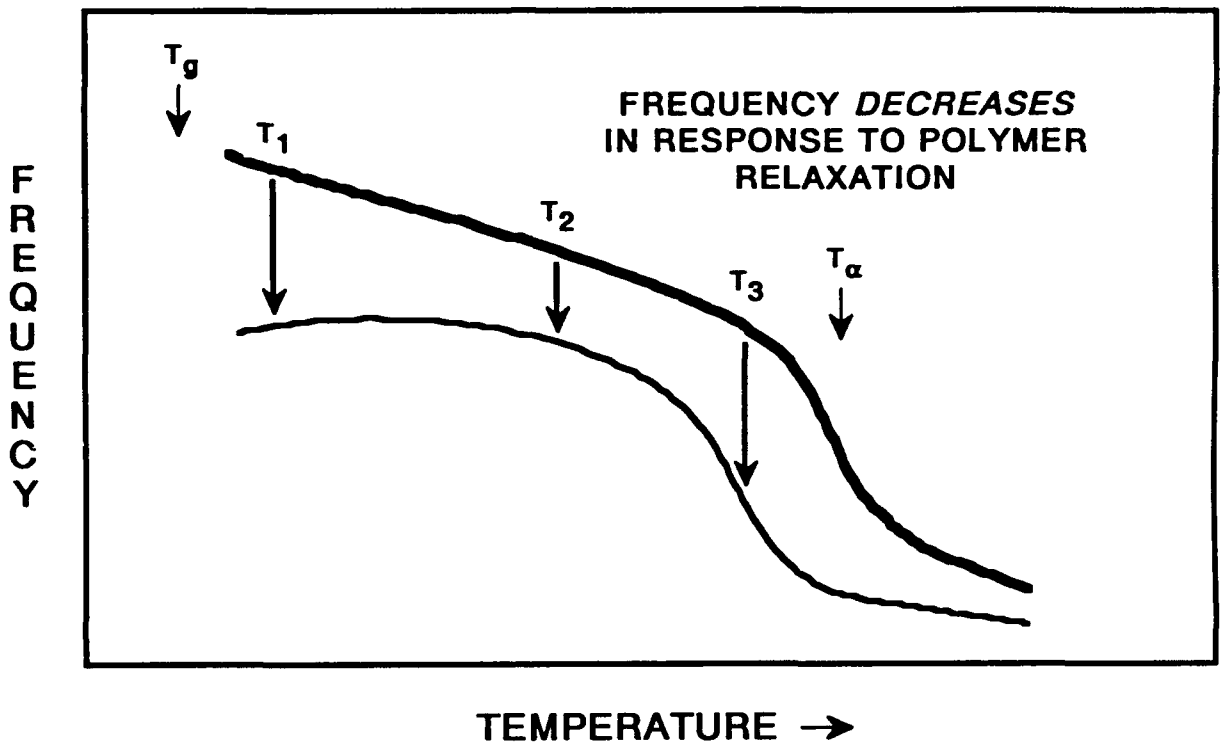


Figure 10. Illustration of a thought experiment where the frequency of a polymer-coated acoustic sensor is monitored as a function of temperature in the absence of a vapor (upper bold curve) and in the presence of a fixed concentration of vapor (lower plain curve). In this case, polymer relaxation processes cause sigmoidal decreases in frequency as has been observed using 5.0 MHz FPW devices.

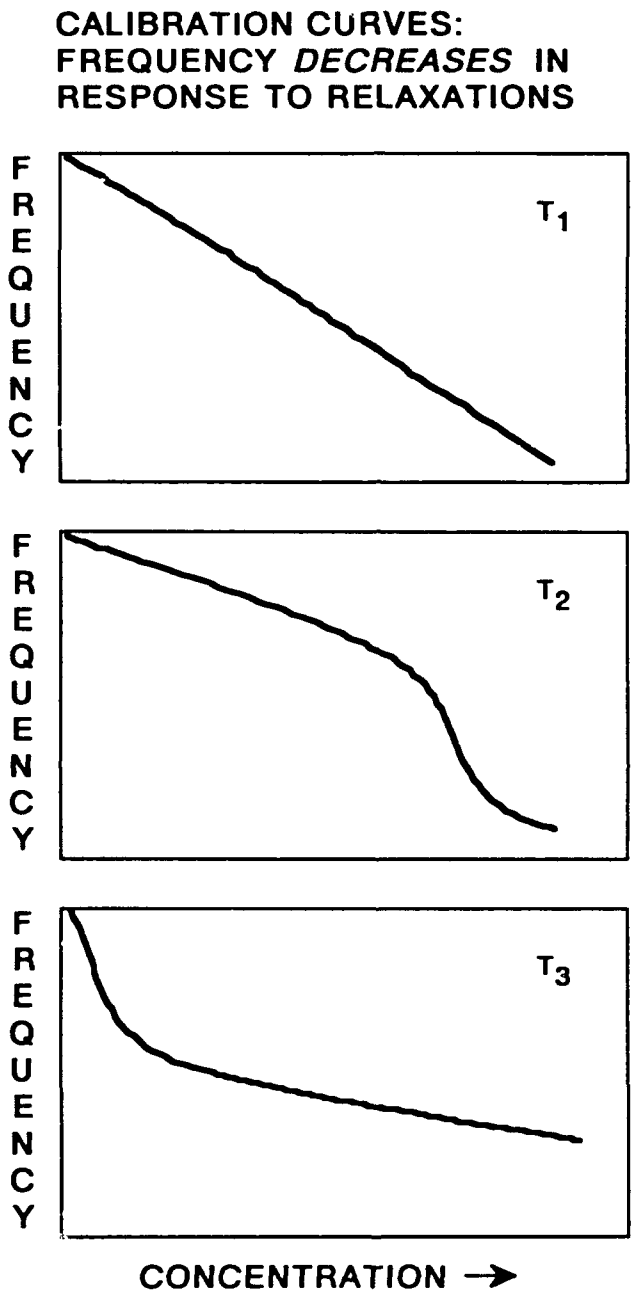


Figure 11. Illustration of the types of calibration curves at three fixed temperatures that would result from the response behavior shown in Figure 10 and described in the text.

These thought experiments clearly show that knowledge of $T_\alpha$ can be important to the interpretation of sensor responses. A calibration curve such as that in the lowest plot of Figure 11 would appear to indicate a curved sorption isotherm and selective vapor-coating interactions at a finite number of specific sites in the polymer. But our arguments show that this shape could arise from relaxation effects. The two possibilities can only be distinguished if the relaxation behavior of the polymer is known (for example by the types of experiments described above) or if the sorption isotherm is known. In addition, these thought experiments illustrate how one could deliberately use relaxation processes to enhance sensor sensitivity within concentration ranges of particular interest. If trace detection were most important, then one would choose a device frequency, polymer, and sensor operating temperature, $T_{sensor}$, so that $T_{sensor}$ was just below $T_\alpha$ (i.e., as shown for $T_3$ in Figure 10). Alternatively, if an alarm level at an intermediate concentration were desirable, one might select $T_{sensor}$ so that $T_{sensor} = T_\alpha$ at the alarm concentration. Then the calibration curve would be steepest through the concentration where the alarm was desired.

The results are quite different and a bit more complicated if the relaxation process causes sensor frequencies to increase, opposing the normal response. This case is illustrated by the hypothetical plots shown in Figures 12 and 13. At $T_1 << T_\alpha$, a normal response is observed and the calibration curve is linear. By contrast, at $T_3$ near $T_\alpha$, the plasticizing effect of the sorbed vapor increases the frequency. This effect could exceed the normal response, causing an observed response in the opposite of the normal direction. We will refer to such a response as an "anomalous" response. In this case, the calibration curve looks like the third one in Figure 13. The frequency increases at low vapor concentrations until $T_\alpha < T_3$, then further mass loading causes the calibration curve to turn down toward the normal direction. *In fact, this type of anomalous calibration curve has been reported* for the sorption of methanol into cured polyimide films on a 97 MHz SAW device at 25°C (46). Our thought experiment provides a possible explanation for these results. Similar results have been reported for pentane sorbing into styrene-butadiene-styrene triblock copolymer on a 97 MHz SAW device at 25°C (36). These data were plotted in a parametric form (in reference 36) rather than as a standard calibration curve, but if one follows the velocity changes only, they correspond in form to the third plot in Figure 13 at all but the lowest pentane concentrations.

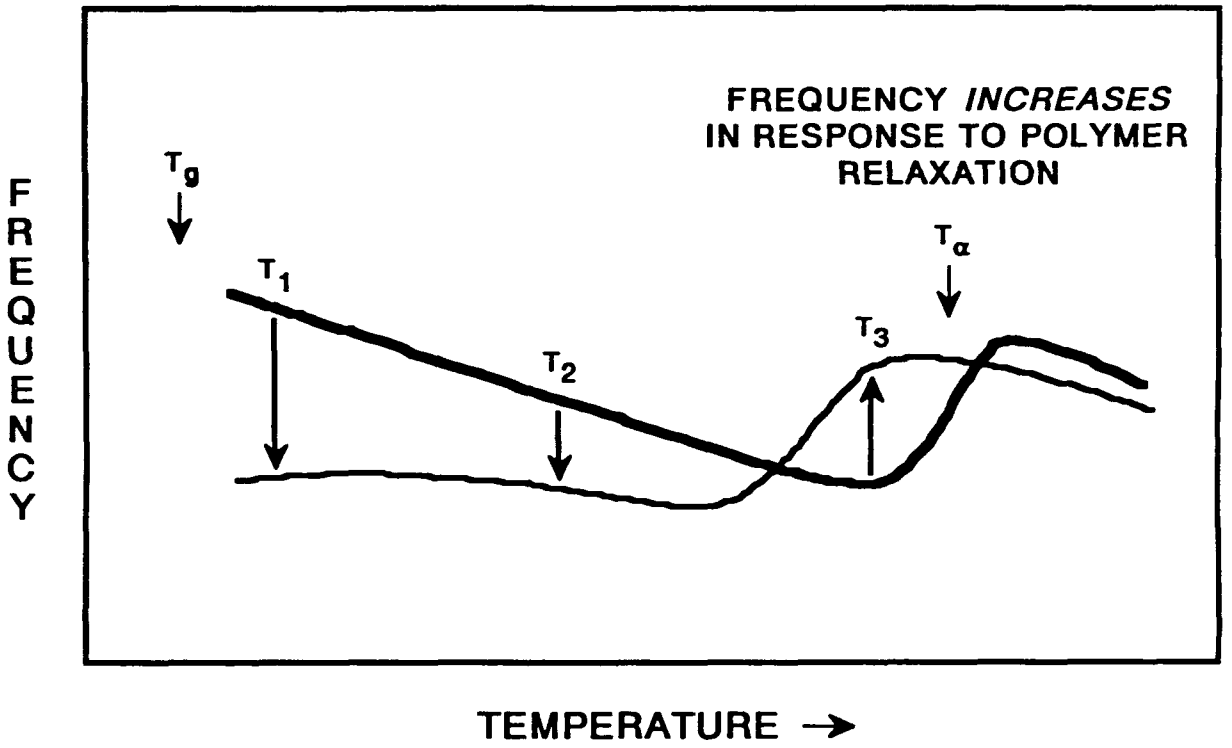


Figure 12. Illustration of a thought experiment where the frequency of a polymer-coated acoustic sensor is monitored as a function of temperature in the absence of a vapor (upper bold curve) and in the presence of a fixed concentration of vapor (lower plain curve). In this case, polymer relaxation processes cause sigmoidal increases in frequency as has been observed on some high-frequency SAW sensors.

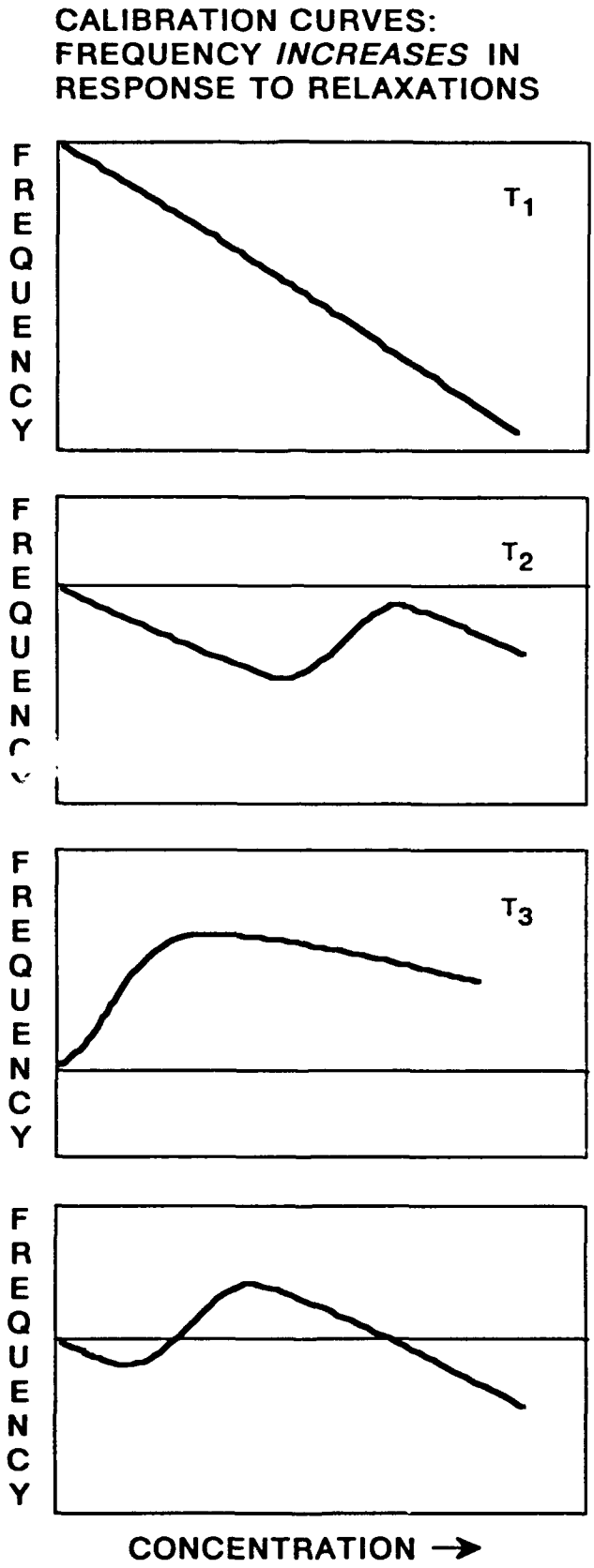


Figure 13. Illustrations of the types of calibration curves at fixed temperatures that would result from the response behavior shown in Figure 12 and described in the text.

The case becomes more complicated at temperature $T_2$. The response is normal until sufficient vapor is sorbed to shift $T_\alpha$ to $T_2$, at which point the calibration curve reverses direction. At sufficiently high vapor concentrations, with $T_\alpha$ shifted well below $T_2$, the calibration curve might reverse direction again. This type of curve is shown in the second plot in Figure 13. Depending on the specifics of the case, the direction changes indicated could cause the curves to intersect with the abscissa, as is shown in the last plot of Figure 13. This calibration curve goes beyond anomalous, possibly to the bizarre, but it is not unrealistic. These types of curves could also arise when the sensor is at $T_3$ if the normal response exceeds the relaxation response at low vapor concentrations. Curves with these characteristics have been reported for the sorption of dibromomethane and trichloroethylene in styrene-butadiene-styrene triblock copolymer on a 97 MHz SAW device at 25°C (36).

In cases like these, a knowledge of polymer relaxation behavior is critical to the rationalization of unusual sensor responses. For example, consider the same polymer applied to two different acoustic devices. On exposing both sensors at the same temperature to the same vapor at the same concentration, one gives a normal response and the other gives an anomalous response. It would appear that the polymer behavior is irreproducible. However, if the acoustic devices are operating at two different frequencies, and relaxation processes are occuring, then such results may be entirely valid. The relaxation processes are frequency-dependent and therefore polymer behavior and sensor responses should be expected to be different on devices of different frequencies.

In addition, this knowledge could be used to select polymers to obtain the desired sensor characteristics. If one wished to avoid anomalous responses, then one would select a polymer such that $T_{sensor}$ was above $T_g$ but very far below $T_\alpha$ (i.e., like $T_1$ in the figures). (Of course, if $\beta$ relaxation processes occur between $T_{sensor}$ and $T_\alpha$, and they influence sensor frequency, then this would have to be considered as well.) Alternatively, if the balance between opposing modulus and viscosity effects during a relaxation process is frequency-dependent, then a polymer and a sensor frequency might be selected so that these effects cancel one another out, leaving only the normal response. Another use of this knowledge could be in the selection of sensors for a sensor array , where one might deliberately select some sensors to give normal responses to certain vapors (e.g., hazards to be detected and measured), and other sensors to give anomalous responses to other vapors (e.g., background vapors to be discriminated against), and thus gain selectivity. Martin and Frye have proposed that measurement of both SAW velocity and attenuation during a relaxation process on a single sensor could be used to discriminate among vapors (36).

Based on the above analyses and past work, it is possible to identify a number of factors that must be understood to fully interpret sensor responses. These factors also serve as variables that can be controlled to design sensors that have particular characteristics: the acoustic device and its operating frequency, the operating temperature of the sensor, the transition behavior(s) of the polymer coating material at the sensor frequency (including the transition types and the temperatures at which they occur), the effects of these transitions on sensor signals (does the frequency decrease, increase, or is it unaffected?), the sorption isotherm of the target analyte into the selected polymer at the sensor temperature, the sorption characteristics of other potentially interfering vapors, and the effect of the vapors on the polymer transition behaviors. The types of experiments described in this paper, including the thought experiments in this discussion, provide methodologies that can be used to systematically explore sensor/polymer/vapor systems where relaxation processes occur.

It is also noteworthy that the FPW experiments provide results that are very similar to those of conventional bulk-wave ultrasonic measurements on polymers, at least with regard to $\alpha$ relaxations. The FPW device provides a simple and convenient method of making these measurements on tiny samples. Sample preparation is trivial: we simply dissolved the sample in solvent and airbrushed it onto the membrane while monitoring freqeuncy to control the film thickness. Automation of the frequency and attenuation measurements is straightforward. Moreover, only one transducer is required and it is in direct contact with the sample. This compares favorably with conventional bulk-wave ultrasonic methods that usually require two transducers, These transducers are separated from the sample by an immersion liquid or buffer rods, leading to multiple interfaces where sound reflection occurs (29,30). Furthermore, in the buffer rod technique, multiple interfaces exist where good bonding must be maintained. In the FPW technique there is only the polymer/membrane interface to be concerned with. With further theoretical development, signal processing, and perhaps new device designs, it may be possible to develop the FPW technique so that fundamental polymer properties can be determined from FPW frequency and attenuation measurements.

## ACKNOWLEDGEMENTS

The authors would like to acknowledge illuminating discussions with Stephen J. Martin and Charles M. Roland, and helpful comments on the manuscript from Robert Y. Ting and Roger N. Capps.

This work was supported (at NRL) by the Office of Naval Technology / Naval Surface Warfare Center, Dahlgren, VA, and (at Berkeley) by the Berkeley Sensor and Actuator Center, a National Science Foundation / Industry / University Cooperative Research Center.

## REFERENCES


1. Costello, B.J; Wenzel, S.W.; Wang, A.; White, R.M., *IEEE Ultrasonics Symposium,* December 5-7, 1990, Honolulu, HI.

2. Moroney, R.M.; White, R.M.; Howe, R.T., *IEEE Ultrasonics Symposium,* December 5-7, 1990, Honolulu, HI.

3. Wenzel, S.W.; White, R.M. *Sens. Actuators* **1990**, *A21-A23,* 700-703.

4. Martin, B.A.; Wenzel, S.W.; White, R.M. *Sens. Actuators* **1990**, *A21-A23,* 704-708.

5. Wenzel, S.W.; White, R.M. *Appl. Phys. Lett.* **1989**, *54*, 1976-1978.

6. White, R.M.; Wenzel, S.W. *Appl. Phys. Lett.* **1988**, *52*, 1653-1655.

7. Wenzel, S.W.; White, R.M. *IEEE Trans. Electron Devices* **1988**, *35*, 735-743.

8. White, R.M.; Wicher, P.J.; Wenzel, S.W.; Zellers, E.T. *IEEE Trans. Ultrason., Ferroelectrics, Freq. Contr.* **1987**, *UFFC-34*, 162-171.

9. Grate, J.W.; Wenzel, S.W.; White, R.M., *Anal. Chem.* **1991** in the press.

10. King, W.H. *Anal. Chem.* **1964**, *36*, 1735-1739.

11. McCallum, J.J. *Analyst(London)* **1989**, *114*, 1173-1189.

12. Wohltjen, H.; Dessy, R.E. *Anal. Chem.* **1979**, *51*, 1458-1475.

13. Wohltjen, H. *Sens. Actuators* **1984**, *5*, 307-325.

14. Fox, C.G.; Alder, J. F. *Analyst(London)* **1989**, *114*, 997-1004.

15. Ballantine, D.S., Jr.; Wohltjen, H. *Anal. Chem.* **1989**, *61*, 704A-715A.

16. D'Amico, A.; Verona, E. *Sens. Actuators* **1989**, *17*, 55-66.

17. Nieuwenhuizen, M.S.; Venema, A. *Sensors and Materials* **1989**, *5*, 261-300.

18. Bastiaans, G.J. *Chemical Sensors*; Edmonds, T.E. Ed.; Blackie: Glasgow and London, **1988**, 295-319.

19. Grate, J.W.; Abraham, M. H. *Sens. Actuators* **1991**, in the press.

20. Roe, R.-J. in *Encyclopedia of Polymer Science and Engineering*, Vol 7, 2nd Ed., John Wiley and Sons, Inc.: New York, 1987; pp 531-544.

21. Wrasidlo, W. in *Advances in Polymer Science*, Vol. 13, Springer-Verlag: New York, 1974; pp 29-53.

22. *Polymer Handbook*, 3rd Ed., John Wiley and Sons, Inc.: New York, 1989.

23. Lewis, O.G. *Physical Constants of Homopolymers*, Springer Verlag: New York, 1968.

24. Lewis, A.F. *Polymer Letters* **1963**, *1*, 649-644.

25. Aklonis, J.J.; MacKnight, W.J.; Shen, M. *Introduction to Polymer Viscoelasticity*, Wiley-Interscience: New York, 1972

26. Ferry, J.D. *Viscoelastic Properties of Polymers*, 3rd. Ed. John Wiley and Sons, Inc.: New York, 1980.

27. McCrum, N.G.; Read, B.E.; Williams, G. *Anelastic and Dielectric Effects in Polymeric Solids*, John Wiley and Sons: New York, 1967.

28. Capps, R.N. *Elastomeric Materials for Acoustic Applications*, Naval Research Laboratory: Washington, D.C., 1989.

29. Massines, R.; Piche, L.; Lacabanne, C. *Makromol. Chem., Macromol. Symp.* **1989**, *23*, 121-137.

30. Hartman, B. in *Encyclopedia of Polymer Science and Engineering*, Vol 1, 2nd Ed., John Wiley and Sons, Inc.: New York, 1984; pp 131-160.

31. Work, R. *J. Appl. Phys.* **1956**, *27*, 69-72.

32. Wada, Y.; Yamamoto, K. *J. Phys. Soc. Jpn.* **1956**, *11*, 887-892.

33. Kwan, S.F.; Chen, F.C.; Choy, C.L. *Polymer* **1975**, *16*, 481-488.

34. Groetsch, J.A., III; Dessy, R.E. *J. Appl. Poly. Sci.* **1983**, *28*, 161-178.

35. Ballantine, D. S., Jr.; Wohltjen, H. in *Chemical Sensors and Microinstrumentation*, ACS Symposium Series 403, American Chemical Society: Washington, D.C., 1989; pp 222-236.

36. Martin, S.J.; Frye, G.C. *Appl. Phys. Lett.* **1990**, *57*, 1867-1869.

37. Lindemann, M.K. in *Encyclopedia of Polymer Science and Technology*, Vol 15, John Wiley and Sons, Inc.: New York, 1971; pp 577-677.

38. Kine, B.B.; Novak, R. W. in *Encyclopedia of Polymer Science and Engineering*, Vol 1, 2nd Ed., John Wiley and Sons, Inc.: New York, 1984; p 257.

39. Shetter, J.A. *J. Poly. Sci. Part B* **1963**, *1*, 209-219.

40. Kanig, G. *Kolloid Z. Z. Polym.* **1969**, *233*, 829-845.

41. Ivey, D.G.; Mrowca, B.A.; Guth, E. *J. Appl. Phys.* **1949**, *20*, 486-492.

42. Thurn, H.; Wolf, K. *Kolloid Z.* **1956**, *148*, 16-30.

43. Nolle, A.W.; Mowry, S.C. *J. Acoust. Soc. Am.* **1948**, *20*, 432-439.

44. Phillips, D.W.; Pethrick, R.A. *J. Macromol. Sci. - Rev. Macromol. Chem.* **1977-78**, *C16*, 1-22.

45. Piche, L. *Ultrasonics Symp. Proc.* **1989**, 599-608.

46. Frye, G.C.; Martin, S.J.; Ricco, A.J. *Sensors and Materials* **1989**, *1*, 335-357.